J|A|C|S
ARTICLES
Published on Web 04/09/2004

Mechanism of Host−Guest Complexation by Cucurbituril

César Márquez,[†] Robert R. Hudgins,[‡] and Werner M. Nau*,[†]

Contribution from the School of Engineering and Science, International University Bremen, Campus Ring 1, D-28759 Bremen, Germany, and the Department of Chemistry, University of Basel, Klingelbergstrasse 80, CH-4056 Basel, Switzerland

Received December 28, 2003; E-mail: w.nau@iu-bremen.de

Abstract: The factors affecting host−guest complexation between the molecular container compound cucurbit[6]uril (CB6) and various guests in aqueous solution are studied, and a detailed complexation mechanism in the presence of cations is derived. The formation of the supramolecular complex is studied in detail for cyclohexylmethylammonium ion as guest. The kinetics and thermodynamics of complexation is monitored by NMR as a function of temperature, salt concentration, and cation size. The binding constants and the ingression rate constants decrease with increasing salt concentration and cation-binding constant, in agreement with a competitive binding of the ammonium site of the guest and the metal cation with the ureido carbonyl portals of CB6. Studies as a function of guest size indicate that the effective container volume of the CB6 cavity is approximately 105 Å^3. It is suggested that larger guests are excluded for two reasons: a high activation barrier for ingression imposed by the tight CB6 portals and a destabilization of the complex due to steric repulsion inside. For example, in the case of the nearly spherical azoalkane homologues 2,3-diazabicyclo[2.2.1]hept-2-ene (DBH, volume ca. 96 Å^3) and 2,3-diazabicyclo[2.2.2]oct-2-ene (DBO, volume ca. 110 Å^3), the former forms the CB6 complex promptly with a sizable binding constant (1300 M^{-1}), while the latter does not form a complex even after several months at optimized complexation conditions. Molecular mechanics calculations are performed for several CB6/guest complexes. A qualitative agreement is found between experimental and calculated activation energies for ingression as a function of both guest size and state of protonation. The potential role of constrictive binding by CB6 is discussed.

Introduction

The inclusion of guest molecules into the cavities of supramolecular hosts with molecular container properties has the potential to allow novel chemical transformations, to mimic enzymatic activity, to isolate reactive species, and to promote uncommon spectroscopic effects.[1−4] Many molecular-container-type hosts such as cyclodextrins and calixarenes allow a fast exchange of the guest, due to their unobstructed openings.[5−9] Carcerands and hemicarcerands, on the other hand, provide large steric or "physical" barriers toward guest exchange, which commonly require elevated temperature to be surmounted.[10,11] This phenomenon, which is known as constrictive binding and which enhances the persistence of the related complexes dramatically, has been systematically examined for (hemi)carcerands.[12−14] In a preliminary communication,[15] we have suggested that a constrictive binding applies also to cucurbit[*n*]urils (CBn) as an alternative class of cagelike macrocyclic structures.

The popularity of cucurbiturils has grown substantially in recent years. The most common derivative is cucurbit[6]uril[16−23] (CB6), which is based on six units of glycoluril enlaced by methylene groups. In its function as a molecular container, CB6 offers a 5.5 Å wide and 6.0 Å high cavity, which is accessible by two "portals" composed of a rim of ureido carbonyl groups.[17,18] These tight portals (ca. 4.0 Å diameter)[17,18] can lead to a constrictive binding. With respect to applications, CB6 has been successfully used in catalytic processes,[24,25] in the con-

[†] International University Bremen and University of Basel.
[‡] University of Basel. Present address: Department of Chemistry, York University, Toronto ON M3J 1P3, Canada.

(1) Cram, D. J. *Nature* **1992**, *356*, 29−36.
(2) Cram, D. J.; Tanner, M. E.; Thomas, R. *Angew. Chem., Int. Ed. Engl.* **1991**, *30*, 1024−1027.
(3) Tucci, F. C.; Renslo, A. R.; Rudkevich, D. M.; Rebek, J., Jr. *Angew. Chem., Int. Ed.* **2000**, *39*, 1076−1079.
(4) Wash, P. L.; Renslo, A. R.; Rebek, J., Jr. *Angew. Chem., Int. Ed.* **2001**, *40*, 1221−1222.
(5) Lucarini, M.; Luppi, B.; Pedulli, G. F.; Roberts, B. P. *Chem. Eur. J.* **1999**, *5*, 2048−2054.
(6) Yoshida, N. *J. Chem. Soc., Perkin Trans. 2* **1995**, *12*, 2249−2256.
(7) Zhang, X.; Gramlich, G.; Wang, X.; Nau, W. M. *J. Am. Chem. Soc.* **2002**, *124*, 254−263.
(8) Nau, W. M.; Zhang, X. *J. Am. Chem. Soc.* **1999**, *121*, 8022−8032.
(9) Izatt, R. M.; Pawlak, K.; Bradshaw, J. S. *Chem. Rev.* **1995**, *95*, 2529−2586.
(10) Houk, K. N.; Nakamura, K.; Sheu, C. M.; Keating, A. E. *Science* **1996**, *273*, 627−629.
(11) Wang, X.; Houk, K. N. *Org. Lett.* **1999**, *1*, 591−594.
(12) Quan, M. L. C.; Cram, D. J. *J. Am. Chem. Soc.* **1991**, *113*, 2754−2755.
(13) Cram, D. J.; Tanner, M. E.; Knobler, C. B. *J. Am. Chem. Soc.* **1991**, *113*, 7717−7727.
(14) Cram, D. J.; Blanda, M. T.; Paek, K.; Knobler, C. B. *J. Am. Chem. Soc.* **1992**, *114*, 7765−7773.
(15) Marquez, C.; Nau, W. M. *Angew. Chem., Int. Ed.* **2001**, *40*, 3155−3160.
(16) Behrend, R.; Meyer, E.; Rusche, F. *Liebigs Ann. Chem.* **1905**, *339*, 1−37.
(17) Freeman, W. A.; Mock, W. L.; Shih, N. Y. *J. Am. Chem. Soc.* **1981**, *103*, 7367−7368.
(18) Mock, W. L. *Top. Curr. Chem.* **1995**, *175*, 1−24.
(19) Jeon, Y. M.; Kim, J.; Whang, D.; Kim, K. *J. Am. Chem. Soc.* **1996**, *118*, 9790−9791.
(20) Buschmann, H.-J.; Cleve, E.; Schollmeyer, E. *Inorg. Chim. Acta* **1992**, *193*, 93−97.
(21) Cintas, P. *J. Inclusion Phenom. Mol. Recognit. Chem.* **1994**, *17*, 205−220.
(22) Kölbel, M.; Menger, F. M. *Adv. Mater.* **2001**, *13*, 1115−1119.
(23) Elemans, J. A. A. W.; Rowan, A. E.; Nolte, R. J. M. *Ind. Eng. Chem. Res.* **2000**, *39*, 3419−3428.
(24) Mock, W. L.; Shih, N. Y. *J. Org. Chem.* **1983**, *48*, 3619−3620.

10.1021/ja0319846 CCC: $27.50

struction of polyrotaxanes,[26−30] supramolecular switches,[31] catenanes,[32] and fluorescent materials,[33,34] and in the removal of contaminants such as colorants[35,36] from water or volatile organic molecules from air.[37]

In addition to CB6, the smaller and larger cyclic glycoluril oligomers CB5, CB7, and CB8 have been described,[38,39] as well as some derivatives soluble in organic solvents such as decamethylcucurbit[5]uril,[40] derivatives with five and six fused cyclohexane rings,[41] and perhydroxycucurbit[*n*]urils.[42] Detailed studies on the oligomerization mechanisms[43−46] allowed the rational design of asymmetric cucurbiturils[47] and tailor-made cucurbituril analogues with different sizes, shapes, and colors.[48] The various applications of the derivatives and their molecular recognition properties have been summarized.[39] CB5 derivatives, for example, complex lead ions selectively,[49] while CB7 has been employed to study electrochemically active complexes[50−52] and to discriminate fluorescence quenching mechanisms.[53] Note also that we have recently explored the physical properties of the larger CB7 by including a solvato-sensitive chromophore. The polarizability of the CB7 cavity was found to be extremely low,[54] in contrast to the exceptionally high polarizability of hemicarcerands,[55] supporting Cram's hypothesis that the inside of molecular container molecules can behave like a new phase of matter.[1,2]

The host−guest complexes between CB6 and alkylammonium ions in acid−water solution,[17,56,57] as well as neutral guests in the presence of salts,[19,58,59] have been studied. Several different modes of intermolecular interactions promote the binding of guests by cucurbiturils. First, like for cyclodextrins, a hydrophobic effect applies, i.e., a composite effect derived from an interplay between the release of "high-energy water" upon complexation of nonpolar organic residues and concomitant differential dispersion interactions inside the cavity and in bulk water.[60,61] Second, ion−dipole interactions of metal cations[20,62] or organic ammonium ions[57,63] with either ureido carbonyl rim may come into play, while hydrogen-bonding interactions prevail less frequently.[64] As a peculiarity, the complexation of metal cations at the ureido rims (which is often required to enhance solubility) can lead to ternary supramolecular complexes composed of host, included guest, and associated metal ion. In fact, it has been suggested that the cations function as "lids" to seal the portal and promote binding.[19,58]

Despite the growing interest in host−guest complexation processes involving cucurbiturils and their applications, relatively little is known about the precise complexation mechanisms with ammonium ions and neutral guests[59,62] and the quantitative effects of the metal cation "lids" on the inclusion of the guest.[52,65] In particular, while the binding affinity of alkali ions and their effect on dissolving CB6 has been studied,[20,35,66−68] the interplay between the association of metal ions and the inclusion of organic ammonium salts has not been investigated in detail, i.e., by studying the kinetics to obtain information on the elementary reaction steps. This is important for the numerous practical applications, which have been proposed. Previously, we have communicated results on the pH-dependent kinetics of ammonium ion complexation by CB6, which has led to the mechanistic involvement of association complexes of ammonium ions, in addition to inclusion complexes.[15] In the present joint kinetic and thermodynamic study, we have investigated the quantitative effect of metal ions on complexation, the cavity size, and the phenomenon of constrictive binding by studying the effects of temperature, guest volume, salt concentration, and cation size and by performing molecular mechanics calculations on host−guest complexation by CB6.

Experimental Section

Materials. Commercial (Fluka) cyclohexylmethylamine (**c6**) was dissolved in diethyl ether, and D_2SO_4 was added dropwise. Cyclohexylmethylammonium sulfate (**c6**H^+) was obtained as a white, spectroscopically pure precipitate and was used after recrystallization from 1:1 MeOH/diethyl ether at −20 °C. CB6 (Merck) was used without further purification. The complex CB6·**c6**H^+ was obtained by adding an excess

(25) Tuncel, D.; Steinke, J. H. G. *Chem. Commun.* **1999**, 1509−1510.
(26) Tuncel, D.; Steinke, J. H. G. *Chem. Commun.* **2001**, 253−254.
(27) Meschke, C.; Buschmann, H.-J.; Schollmeyer, E. *Polymer* **1999**, *40*, 945−949.
(28) Schollmeyer, E.; Buschmann, H.-J.; Jansen, K.; Wego, A. *Prog. Colloid Polym. Sci.* **2002**, *121*, 39−42.
(29) Lee, E.; Heo, J.; Kim, K. *Angew. Chem., Int. Ed.* **2000**, *39*, 2699−2701.
(30) Park, K.-M.; Whang, D.; Lee, E.; Heo, J.; Kim, K. *Chem. Eur. J* **2002**, *8*, 498−508.
(31) Mock, W. L. In *Comprehensive Supramolecular Chemistry*; Vögtle, F., Ed.; Elsevier Press: New York, 1996; Vol. 2, pp 477−493.
(32) Roh, S. G.; Park, K. M.; Park, G. J.; Sakamoto, S.; Yamaguchi, K.; Kim, K. *Angew. Chem., Int. Ed.* **1999**, *38*, 638−641.
(33) Wagner, B. D.; MacRae, A. I. *J. Phys. Chem. B* **1999**, *103*, 10114−10119.
(34) Wagner, B. D.; Fitzpatrick, S. J.; Gill, M. A.; MacRae, A. I.; Stojanovic, N. *Can. J. Chem.* **2001**, *79*, 1101−1104.
(35) Buschmann, H.-J.; Schollmeyer, E. *Textilveredlung* **1993**, *28*, 182−184.
(36) Buschmann, H.-J.; Schollmeyer, E. *J. Inclusion Phenom. Mol. Recognit. Chem.* **1992**, *14*, 91−99.
(37) Dantz, D. A.; Meschke, C.; Buschmann, H.-J.; Schollmeyer, E. *Supramol. Chem.* **1998**, *9*, 79−83.
(38) Kim, J.; Jung, I. S.; Kim, S. Y.; Lee, E.; Kang, J. K.; Sakamoto, S.; Yamaguchi, K.; Kim, K. *J. Am. Chem. Soc.* **2000**, *122*, 540−541.
(39) Lee, J. W.; Samal, S.; Selvapalam, N.; Kim, H.-J.; Kim, K. *Acc. Chem. Res.* **2003**, *36*, 621−630.
(40) Flinn, A.; Hough, G. C.; Stoddart, J. F.; Williams, D. J. *Angew. Chem., Int. Ed. Engl.* **1992**, *31*, 1475−1477.
(41) Zhao, J.; Kim, H.-J.; Oh, J.; Kim, S.-Y.; Lee, J. W.; Sakamoto, S.; Yamaguchi, K.; Kim, K. *Angew. Chem., Int. Ed.* **2001**, *40*, 4233−4235.
(42) Jon, S. Y.; Selvapalam, N.; Oh, D. H.; Kang, J.-K.; Kim, S.-Y.; Jeon, Y. J.; Lee, J. W.; Kim, K. *J. Am. Chem. Soc.* **2003**, *125*, 10186−10187.
(43) Wu, A.; Chakraborty, A.; Witt, D.; Lagona, J.; Damkaci, F.; Ofori, M. A.; Chiles, J. K.; Fettinger, J. C.; Isaacs, L. *J. Org. Chem.* **2002**, *67*, 5817−5830.
(44) Chakraborty, A.; Wu, A.; Witt, D.; Lagona, J.; Fettinger, J. C.; Isaacs, L. *J. Am. Chem. Soc.* **2002**, *124*, 8297−8306.
(45) Burnett, C. A.; Lagona, J.; Wu, A.; Shaw, J. A.; Coady, D.; Fettinger, J. C.; Day, A. I.; Isaacs, L. *Tetrahedron* **2003**, *59*, 1961−1970.
(46) Day, A.; Arnold, A. P.; Blanch, R. J.; Snushall, B. *J. Org. Chem.* **2001**, *66*, 8094−8100.
(47) Isobe, H.; Sato, S.; Nakamura, E. *Org. Lett.* **2002**, *4*, 1287−1289.
(48) Lagona, J.; Fettinger, J. C.; Isaacs, L. *Org. Lett.* **2003**, *5*, 3745−3747.
(49) Zhang, X. X.; Krakowiak, K. E.; Xue, G.; Bradshaw, J. S.; Izatt, R. M. *Ind. Eng. Chem. Res.* **2000**, *39*, 3516−3520.
(50) Ong, W.; Gómez-Kaifer, M.; Kaifer, A. E. *Org. Lett.* **2002**, *4*, 1791−1794.
(51) Kim, H.-J.; Jeon, W. S.; Ko, Y. H.; Kim, K. *Proc. Natl. Acad. Sci. U.S.A.* **2002**, *99*, 5007−5011.
(52) Moon, K.; Kaifer, A. E. *Org. Lett.* **2004**, *6*, 185−188.
(53) Marquez, C.; Pischel, U.; Nau, W. M. *Org. Lett.* **2003**, *5*, 3911−3914.
(54) Marquez, C.; Nau, W. M. *Angew. Chem., Int. Ed.* **2001**, *40*, 4387−4390.
(55) Pina, F.; Parola, A. J.; Ferreira, E.; Maestri, M.; Armaroli, N.; Ballardini, R.; Balzani, V. *J. Phys. Chem.* **1995**, *99*, 12701−12703.
(56) Mock, W. L.; Shih, N. Y. *J. Org. Chem.* **1986**, *51*, 4440−4446.
(57) Mock, W. L.; Shih, N. Y. *J. Am. Chem. Soc.* **1989**, *111*, 2697−2699.
(58) Whang, D.; Heo, J.; Park, J. H.; Kim, K. *Angew. Chem., Int. Ed.* **1998**, *37*, 78−80.
(59) El Haouaj, M.; Ko, Y. H.; Luhmer, M.; Kim, K.; Bartik, K. *J. Chem. Soc., Perkin Trans. 2* **2001**, 2104−2107.
(60) Schmidtchen, F. P. *Chem. Eur. J.* **2002**, *8*, 3522−3529.
(61) Buschmann, H.-J.; Jansen, K.; Schollmeyer, E. *Thermochim. Acta* **1998**, *317*, 95−98.
(62) Hoffmann, R.; Knoche, W.; Fenn, C.; Buschmann, H.-J. *J. Chem. Soc., Faraday Trans.* **1994**, *90*, 1507−1511.
(63) Mock, W. L.; Shih, N. Y. *J. Am. Chem. Soc.* **1988**, *110*, 4706−4710.
(64) Buschmann, H.-J.; Jansen, K.; Schollmeyer, E. *Thermochim. Acta* **2000**, *346*, 33−36.
(65) Kellersberger, K. A.; Anderson, J. D.; Ward, S. M.; Krakowiak, K. E.; Dearden, D. V. *J. Am. Chem. Soc.* **2001**, *123*, 11316−11317.
(66) Karcher, S.; Kornmüller, A.; Jekel, M. *Acta Hydrochim. Hydrobiol.* **1999**, *27*, 38−42.
(67) Buschmann, H.-J.; Jansen, K.; Meschke, C.; Schollmeyer, E. *J. Solution Chem.* **1998**, *27*, 135−140.
(68) Buschmann, H.-J.; Cleve, E.; Jansen, K.; Wego, A.; Schollmeyer, E. *J. Inclusion Phenom. Macrocyclic Chem.* **2001**, *40*, 117−120.

Chart 1

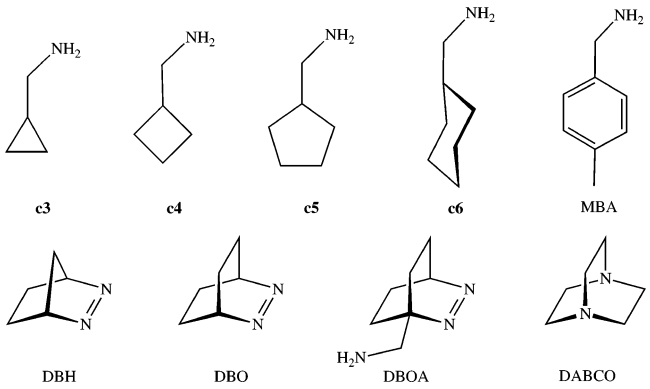

of **c6**H$^+$ to a solution of CB6 in 0.2 M Na_2SO_4 in D_2O; it precipitated slowly as a white powder, and its purity was checked by ^{1}H NMR; no presence of free CB6 was observed. 2,3-Diazabicyclo[2.2.1]hept-2-ene (DBH),[69] 2,3-diazabicyclo[2.2.2]oct-2-ene (DBO),[70] and 1-aminomethyl-2,3-diazabicyclo[2.2.2]oct-2-ene (DBOA)[71] were synthesized according to literature procedures. 1,4-Diazabicyclo[2.2.2]octane (DABCO), standard chemicals, and salts (>98%) were purchased from Fluka or Merck. D_2O (Glaser AG, Basel, Switzerland, > 99% D) was used as received. All experiments were performed at ambient temperature (25 °C) unless otherwise indicated (Chart 1).

Kinetics and Thermodynamics of Complexation. The kinetics and thermodynamics of complexation of the guests by CB6 was studied in D_2O in the presence of different amounts of alkali cations (as chloride salts, with the exception of lithium) or in D_2O/formic acid (1:1, v/v, pH ca. 1.3). Equilibration was achieved either by dissolving previously precipitated and isolated 1:1 complex (ca. 3 mM) or by mixing equimolar amounts (ca. 3 mM) of free host and guest; in some cases, both methods were used to provide a control experiment and evidence for the reversibility of the process. The complexation process was followed with time by NMR spectroscopy on a Bruker DPX 400 MHz or DRX 500 MHz spectrometer. The concentration of free guest was monitored because it gave the most accurate results, due to the well-separated NMR peaks. The spectra were subsequently analyzed with the software package SwaN-MR.[72]

To obtain the rate constants for the formation of CB6·**c6**H$^+$ as host−guest complex (HG) from CB6 as host (H) and **c6**H$^+$ as guest (G), a simple H + G ⇌ HG model was adopted, using the analytical procedure proposed by Mauser.[73] This procedure bypasses the use of different forms of integrated equations for different initial concentration conditions.[74] In the special case of a molecular container compound as host, the association and dissociation rate constants are felicitously referred to as rate constants for ingression and egression, $k_{ingress}$ and k_{egress}.

The general expression for the temporal evolution of the concentration of the complex, [HG], versus time is given by eq 1, where the parameter r depends on the initial conditions ($t = 0$):

$$[HG] = [HG]_\infty + \frac{([HG]_o - [HG]_\infty)re^{-rt}}{r + k_{ingress}([HG]_o - [HG]_\infty)(re^{-rt} - 1)}$$

where

$$r = \sqrt{k_{egress}^2 + 4k_{egress}k_{ingress}[HG]_o} \text{ for } [H]_o = [G]_o = 0$$

and where

$$r = k_{egress} + 2k_{ingress}[G]_\infty \text{ for } [H]_o = [G]_o \text{ and } [HG]_o = 0$$

and where

$$r = \sqrt{(k_{egress} + k_{ingress}([H]_o - [G]_o))^2 + 4k_{egress}k_{ingress}[G]_o} \text{ for } [H]_o \neq [G]_o \text{ and } [HG]_o = 0 \quad (1)$$

The kinetics was studied at different starting conditions and analyzed according to eq 1 with the appropriate r term. The software package ProFit[75] was used for the nonlinear fitting procedures of the rate data; the statistical error obtained by the least-squares method was <10% in all cases.

Binding Constant of CB6·c6H$^+$ in the Absence of Salts. This binding constant (1.1×10^5 M^{-1}) was obtained by adding **c6**H$^+$ (1.5 mM) to a saturated solution of CB6 (in the presence of an excess of undissolved CB6). The amount of complex was determined by ^{1}H NMR spectroscopy in D_2O in the absence of salts. Note that the complex is more soluble than free CB6, thereby "pulling" CB6 into solution. The solubility of CB6 in pure water (required to calculate K) was determined by adding an excess of CB6 to 2.5 L of bidistilled water, heating the solution to reflux for 48 h, and subsequent standing for 1 week at ambient temperature. Filtration, removal of solvent, and weighing the dissolved amount provided a value of 30 μM, which compares with a value of ca. 20 μM reported in the literature.[67,76]

Computational Studies. All computational studies were performed using the Hyperchem[77] and Gaussian 98 packages.[78] The molecular charge distribution of each structure was set according to an initial ab initio geometry optimization at the HF/6-311G** level.[79,80] Conformational searches and geometry optimizations of the host−guest systems were performed within the all-atom MM+ force field[81] and parameter set, using bond dipoles (noncharged guests) or partial atomic charges (charged guests) for the calculation of nonbonded electrostatic interactions. The conformational search option in HyperChem was used to search the potential energy surfaces for energy minima. Each minimum was conjugate-gradient-minimized to ≤0.05 kcal Å^{-1} mol^{-1}, and the energy of the lowest energy geometry is reported. The same criteria were adopted in the stepwise constrained geometry optimizations for the host−guest egression calculations.

The calculations suggest that the D_{6h} structure of CB6 is not the gas-phase minimum, due to the large internal cavity. Instead, a less symmetric collapsed form is the minimum, which presumably allows for some additional dispersion interactions between the walls without a significant increase in strain energy. Nevertheless, to reduce ambiguity, the D_{6h} CB6 structure was selected as a starting geometry and reference structure. Volume calculations were performed within the Quantitative Structure−Activity Relationships (QSAR) Module of HyperChem.

(69) Cohen, S. G.; Steel, C.; Zand, R. *J. Am. Chem. Soc.* **1961**, *83*, 2895−2900.
(70) Askani, R. *Chem. Ber.* **1965**, *98*, 2551−2555.
(71) Hudgins, R. R.; Huang, F.; Gramlich, G.; Nau, W. M. *J. Am. Chem. Soc.* **2002**, *124*, 556−564.
(72) SwaN-MR, Ver. 3.2.0, Balacco, G., Menarini Ricerche S.p.A, Florence, Italy.
(73) Mauser, H. *Formale Kinetik*; Bertelsmann Universitätsverlag: Düsseldorf, 1974.
(74) Pladziewicz, J. R.; Lesniak, J. S.; Abrahamson, A. J. *J. Chem. Educ.* **1986**, *63*, 850−851.
(75) proFit, Ver. 5.6.3, QuantumSoft, Zürich, Switzerland.
(76) Buschmann, H. J.; Schollmeyer, E.; Mutihac, L. *Thermochim. Acta* **2003**, *399*, 203−208.
(77) HyperChem, Ver. 6.01, Hypercube, Inc., Gainesville, FL.
(78) Gaussian, Ver. 98: Frisch, M. J.; Trucks, G. W.; Schlegel, H. B.; Scuseria, G. E.; Robb, M. A.; Cheeseman, J. R.; Zakrzewski, V. G.; J. A. Montgomery, J.; Stratmann, R. E.; Burant, J. C.; Dapprich, S.; Millam, J. M.; Daniels, A. D.; Kudin, K. N.; Strain, M. C.; Farkas, O.; Tomasi, J.; Barone, V.; Cossi, M.; Cammi, R.; Mennucci, B.; Pomelli, C.; Adamo, C.; Clifford, S.; Ochterski, J.; Petersson, G. A.; Ayala, P. Y.; Cui, Q.; Morokuma, K.; Salvador, P.; Dannenberg, J. J.; Malick, D. K.; Rabuck, A. D.; Raghavachari, K.; Foresman, J. B.; Cioslowski, J.; Ortiz, J. V.; Baboul, A. G.; Stefanov, B. B.; Liu, G.; Liashenko, A.; Piskorz, P.; Komaromi, I.; Gomperts, R.; Martin, R. L.; Fox, D. J.; Keith, T.; Al-Laham, M. A.; Peng, C. Y.; Nanayakkara, A.; Challacombe, M.; Gill, P. M. W.; Johnson, B.; Chen, W.; Wong, M. W.; Andres, J. L.; Gonzalez, C.; Head-Gordon, M.; Replogle, E. S.; Pople, J. A. Gaussian, Inc., Pittsburgh, PA.
(79) Krishnan, R.; Kinkley, J. S.; Seeger, R.; Pople, J. A. *J. Chem. Phys.* **1980**, *72*, 650−654.
(80) McLean, A. D.; Chandler, G. S. *J. Chem. Phys.* **1980**, *72*, 5639−5648.
(81) Allinger, N. L. *J. Am. Chem. Soc.* **1977**, *99*, 8127−8134.

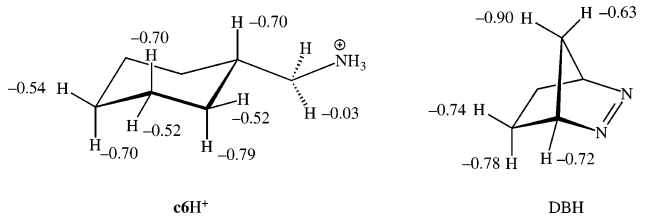

c6H$^+$ DBH

Figure 1. Chemically induced ^{1}H NMR shifts (CIS, in ppm) of **c6**H$^+$ and DBH upon complexation by CB6 in D_2O/formic acid (1:1, v/v) solution, extrapolated to quantitative complexation by using the experimental binding constants.

Results

Formation of Inclusion Complexes and Cavity Size. In the initial studies using organic ammonium ions,[56,82] the cyclopentylmethylammonium (**c5**H$^+$) and 4-methylbenzylammonium (MBAH$^+$) ions were found to be the largest derivatives capable of forming a complex with CB6.[31] The next larger derivative, the cyclohexylmethylammonium ion (**c6**H$^+$), showed no observable complex formation in competitive binding experiments.[21,56] Another experimental study suggests also that the cyclohexyl group serves as a sufficiently large stopper in a diamide chain to sterically prevent the threading of CB6 to form a rotaxane.[83] In recent experiments, however, we have provided evidence for the complexation of **c6**H$^+$ by CB6 with a 1:1 stoichiometry.[15] As shown in Figure 1, the guest protons belonging to CB6·**c6**H$^+$ exhibit the characteristic NMR shielding effect.[18,31] The chemically induced NMR shifts (CIS) compare favorably with the reported CIS values of ca. −1.0 ppm for 1,5-diaminopentane[18] and ca. −0.8 ppm for THF.[19]

The low CIS value of the exocyclic methylene group of **c6**H$^+$ suggests that this group is displaced away from the center and that the ammonium site interacts with the carbonyl oxygens of CB6. In contrast, the cyclohexyl group is deeply immersed, and retains, according to NMR, a chair conformation with an equatorial methylammonium group. Interestingly, a significantly lower CIS value (ca. −0.7 versus −0.5) for the axial protons reflects their closer proximity to the cavity walls; the latter is confirmed by force-field calculated structures (see below). In addition, the upper and lower methylene hydrogens of CB6 display signal splitting upon addition of **c6**H$^+$, which is due to the loss of the equatorial plane of symmetry in the CB6·**c6**H$^+$ complex, see the structure below:

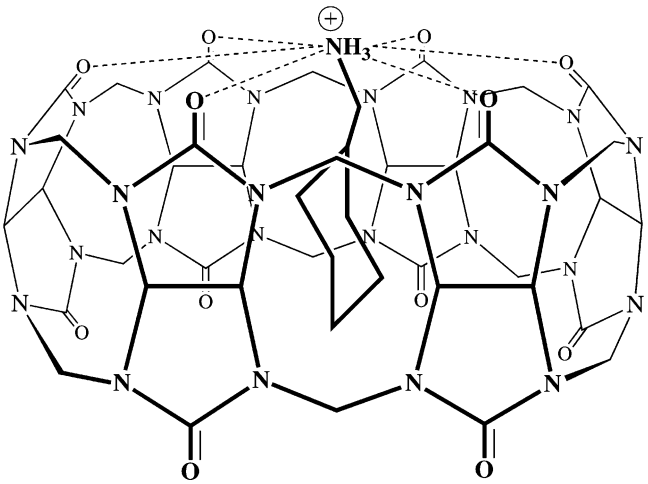

The experiments indicated that the CB6 cavity is capable of encapsulating larger molecules than previously presumed. In an effort to explore the limit of accessible volume in the CB6 cavity, complexation of larger, spherical guest molecules was studied: the bicyclic azoalkanes DBH, DBO, and DBOAH$^+$, as well as DABCO. The choice of the azoalkanes instead of the homologous bicycloalkanes allowed the use of more sensitive UV-spectrophotometric and/or fluorimetric methods for the detection of complexation in addition to NMR.

DBH did in fact undergo complexation with CB6 in D_2O/0.2 M Na_2SO_4 (K = 1300 M^{-1}). The average CIS values of DBH are larger than for **c6**H$^+$ (Figure 1), which is indicative of a tighter fit and closer proximity of the guest protons to the cavity walls. For DBH, no splitting of the CB6 methylene signals was observed, suggesting no preferential conformation of DBH within the cavity on the NMR time scale. Complexation of DBH in CB6 was also observed in D_2O/formic acid (1:1, v/v), but in this case precipitation of the complex occurred. Interestingly, as monitored by NMR, DBH formed the complex with CB6 only in the presence of sodium, but not with the heavier alkali ions (0.2 M); this revealed once more a crucial influence of the metal cation on the complexation process.

Complexation with all larger guests (DBO, DBOAH$^+$, and DABCO) was unsuccessful, although a large range of complexation conditions was employed, including the addition of different salts and the use of formic acid as cosolvent. Even with a large excess of the guest, at elevated temperature (up to 70 °C), or over prolonged time (up to 1 year), no complexation was detected, although binding constants as low as 5 M^{-1} should have been detectable.[15]

Thermodynamics and Kinetics of Complexation. Several CB6 complexes undergo a slow exchange of the guest on the NMR time scale.[18,31] This results in two separate sets of signals when both uncomplexed and complexed species are present, e.g., for **c6**H$^+$ and DBH as guests. In the present study, we have employed **c6**H$^+$ as the primary model to investigate the mechanism of inclusion. Binding constants (K) at various complexation conditions, including different temperatures, were determined by integrating characteristic ^{1}H NMR signals of the free and enclosed species. To ensure equilibration, the signals were followed with time until no change in the relative concentrations was observed. Experiments, in which the equilibrium was either approached by mixing free host and guest, or by dissolving previously precipitated complex, yielded the same results, within error (compare values in brackets in Table 1).

The complexation and decomplexation process was sufficiently slow to follow with time the complexation kinetics through the well-separated NMR signals of free and complexed **c6**H$^+$ (as well as DBH). This allows one to directly extract the rate constants for ingression and egression according to the kinetic analysis outlined in the Experimental Section. The temperature dependence of both the binding constants and rate constants provided the enthalpies and entropies of complexation, in addition to the activation enthalpies and entropies (Tables 2 and 3). The corresponding van't Hoff plots ($\Delta G°/T$ versus $1/T$) were linear over the examined temperature range (25−70 °C).

The data in Tables 2 and 3 show that the complexation of **c6**H$^+$ by CB6 is enthalpy-driven. The complexation entropy is

(82) Meschke, C.; Buschmann, H.-J.; Schollmeyer, E. *Thermochim. Acta* **1997**, *297*, 43−48.
(83) Jansen, K.; Buschmann, H.-J.; Wego, A.; Döpp, D.; Mayer, C.; Drexler, H.-J.; Holdt, H. J.; Schollmeyer, E. *J. Inclusion Phenom. Macrocycl. Chem.* **2001**, *39*, 357−363.

Table 1. Binding Constants and Rate Constants for Inclusion of **c6**H^+ in CB6 at Different Temperatures and in Different Solvents[a]

D_2O with 0.2 M Na_2SO_4				D_2O/formic acid (1:1, v/v)			
T/°C	$10^3 k_{ingress}$/(M^{-1} s^{-1})	$10^5 k_{egress}$/s^{-1}	K/M^{-1}	T/°C	$10^3 k_{ingress}$/(M^{-1} s^{-1})	$10^5 k_{egress}$/s^{-1}	K/M^{-1}
25	0.79	0.48	170 [160][b]	25	0.40	0.31	130
30	1.7	1.2	150 [150][b]	33	0.41	0.45	90
40	8.1	7.3	110 [120][b]	40	0.88	1.1	80
50	31	38	84 [82][b]	48	1.9	2.7	70
60	150	260	58	60	5.2	13	41
				72	14	45	31

[a] Values were obtained by monitoring the decomplexation of previously precipitated and isolated CB6·**c6**H^+ complex (3 mM); error in data is 10%. [b] Values in brackets were obtained by monitoring the complexation of free CB6 with free **c6**H^+.

Table 2. Kinetic and Thermodynamic Parameters for Inclusion of Different Guests in CB6 at 313 K in D_2O/Formic Acid (1:1, v/v)[a]

guest	$10^3 k_{ingress}$/(M^{-1} s^{-1})	$10^5 k_{egress}$/s^{-1}	K/M^{-1}	$H^{\ddagger}_{ingress}$/(kcal mol^{-1})	$H°$/(kcal mol^{-1})	$S°$/(cal K^{-1} mol^{-1})
$MBAH^+$	2700	8.5×10^2	3.2×10^2	13.4 ± 0.4	-5.4 ± 0.2	-5.5 ± 0.5
c3H^+	$\geq 10^9$	$>10^7$	1.5×10^4			
c4H^+	5.9×10^6	1600	3.7×10^5			
c5H^+	5500	1.6	3.3×10^5			
c6H^+	0.88	1.1	8.0×10^1	18.8 ± 0.4	-5.7 ± 0.8	-9.7 ± 2.4

[a] From refs 31, 56, and 57, except for **c6**H^+ (this work).

Table 3. Kinetic and Thermodynamic Parameters for Inclusion of Different Guests in CB6 at 298 K in D_2O with 0.2 M Sodium Sulfate

guest	$10^3 k_{ingress}$/(M^{-1} s^{-1})	$10^5 k_{egress}$/s^{-1}	K/M^{-1}	$H^{\ddagger}_{ingress}$/(kcal mol^{-1})	$H°$/(kcal mol^{-1})	$S°$/(cal K^{-1} mol^{-1})
c6[a]	14.5	145	10	*b*	*b*	*b*
c6H^+	0.81	48	170	29.6 ± 0.5	-5.9 ± 0.4	-9.8 ± 1.3
DBH	1.2	0.09	1300	*c*	*c*	*c*

[a] From ref 15. [b] Activation parameters could not be determined due to very weak binding. [c] Activation parameters could not be determined due to significant thermal decomposition of DBH (elimination of N_2), especially at temperatures >40 °C.

negative, which reflects the formation of a tight complex with a well-defined geometry and high restriction of motion, as expected for the relatively large guest. For comparison, the complexation of $MBAH^+$, which is a more compact aromatic guest (see calculated volumes below), results in a smaller loss of entropy ($S°$ in Table 2). Negative complexation entropies have been previously reported for complexation of large guests with CB6,[36,61,82,84] but positive complexation entropies are more frequently observed.[61,64,76,83,84] The latter are indicative of the release of high-energy water molecules from the host cavity[60] or the desolvation of the guest, which dominates the complexation entropy term unless a very tight complex is formed.

The complexation process was studied as a function of guest size, solvent, and metal ion concentration. The thermodynamics of complexation for **c6**H^+ is compared in Table 2 with previous data[56,62] for the smaller homologues, cyclopentylmethylammonium (**c5**H^+), cyclobutylmethylammonium (**c4**H^+), cyclopropylmethylammonium (**c3**H^+), as well as $MBAH^+$. For consistency, all values in Table 2 refer to experiments in D_2O/formic acid solution at 40 °C. The selection of a different solvent had a large effect on the kinetics and the activation enthalpies, yet only a minor effect on the thermodynamics of complexation (Tables 1−3). For example, in the 25−60 °C temperature range, $k_{ingress}$ increased by more than a factor of 200 in D_2O/Na_2SO_4, while the increase in D_2O/formic acid was only about a factor of 13; consequently, the complexation process displays a significantly higher activation energy in the presence of sodium (compare Tables 2 and 3).

The dependence of the binding constants and complexation kinetics of **c6**H^+ on the cation concentration was studied for sodium (Table 4) and that on the cation *type* was studied for the alkali series (as chlorides, Table 5). The effect of Li^+ could not be studied, due to the low solubility of CB6 with Li^+, which itself signals a weak complexation of this very small and strongly hydrated cation.

Table 4. Binding Constants and Rate Constants for the Inclusion of **c6**H^+ in CB6 in D_2O at Different Salt Concentrations[a]

[Na_2SO_4]/M	$10^3 k_{ingress}$/(M^{-1} s^{-1})	$10^5 k_{egress}$/s^{-1}	K/M^{-1}
0.0	$(4.4 \pm 1.1) \times 10^4$ [b]	0.4 ± 0.1[b]	1.1×10^5 [c]
0.1	1.3	0.39	320
0.2	0.72	0.44	170
0.3	0.49	0.49	100
0.4	0.31	0.38	80
0.5	0.23	0.34	65
0.6	0.17	0.35	50

[a] Measured with [CB6] = 3 mM and [**c6**H^+] = 6 mM; error in data is 10%. [b] Extrapolated from the binding constant by assuming a constant egression rate constant. [c] Calculated by adding a large excess of CB6 to a sample of **c6**H^+ (3 mM) in D_2O; see text.

Table 5. Kinetic and Thermodynamic Parameters for Inclusion of **c6**H^+ in CB6 in the Presence of Different Cations (M^+) in D_2O/Formic Acid (1:1, v/v) at 298 K[a]

M^+	cation radius[b]/Å	K_2[b,c]/M^{-1}	$10^3 k_{ingress}$/(M^{-1} s^{-1})	$10^5 k_{egress}$/s^{-1}	K_{obs}/M^{-1}
Na^+	1.02	1450	0.24	0.51	47
K^+	1.38	560	0.26	0.39	67
Rb^+	1.52	410	0.32	0.38	84
Cs^+	1.70		0.45	0.50	90

[a] Measured with [CB6] = 4 mM, [**c6**H^+] = 8 mM, and [MCl] = 0.5 M; error in data is 10%. [b] From ref 62. [c] Cation binding constant refers to association of the first cation (see Scheme 1).

Molecular Mechanics Calculations. We have selected the MM+ force field implemented in HyperChem, which already contained the required force-field parameters to model the guests

(84) Buschmann, H.-J.; Jansen, K.; Schollmeyer, E. *J. Inclusion Phenom. Macrocycl. Chem.* **2000**, *37*, 231−236.

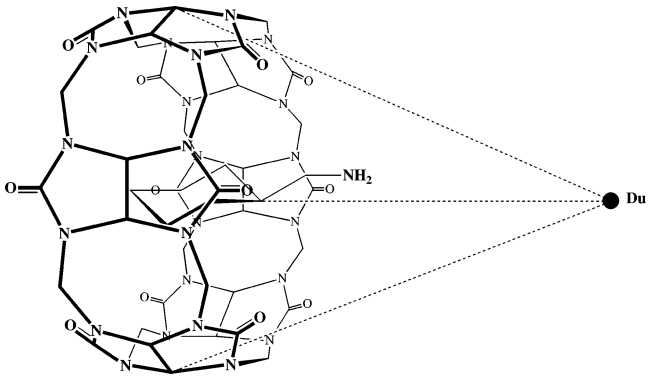

Figure 2. Reaction coordinate used in the force-field calculations of the complexation process for organic guest molecules by CB6; the distance between host and guest was varied along an axial trajectory and defined relative to the fixed position of a dummy atom (Du).

and CB6. The related MM3 force field, which as with MM+, is derived from the original Allinger force field,[81] has already proven useful to predict trends in the complexation energies of hemicarcerands.[85,86] All simulations were done in the gas phase in the presence of host and guest only. Complexed cations at the portals of the host were not included, since their addition was unlikely to yield meaningful information in the absence of an appropriate solvation model.

We assumed that the pathways for ingression and egression are the same (microscopic reversibility) and have therefore only modeled one process, that of egression. We used an approach similar to that described by Sheu and Houk for hemicarcerands.[85,86] Following a complete geometry and energy minimization of the host−guest complex, the activation energies for guest egression from the inner cavity of CB6 were calculated by defining a complexation coordinate (Figure 2) coinciding with the CB6 rotational symmetry axis, along which the guest could be forced in 0.25-Å increments from the center of the cavity (≡ 0 Å distance) through the portals (ca. 3 Å) into free space (≡ 15 Å). To achieve this, the position of a dummy atom (Du) was fixed and a force constant of 7 millidynes Å^{-1} was imposed relative to all central carbons of the host.[15] The distance between host and guest was then varied indirectly by varying the distance between the bridge carbon of the respective guest and the dummy atom by imposing a force constant of 15 millidynes Å^{-1}. Geometry optimizations within these constraints provided the potential energy at each step. It should be noted that both the guest and host structure were optimized during the complexation process; expectedly, the more spherical guests required a movement of all carbonyl groups during inclusion (reminiscent of the opening of a flower), while for the aromatic and cycloalkyl guests an unsymmetrical distortion of the portal was preferred.

Expectedly, the energies were highest when the guest was positioned between the tight portals of the host, and the maximum value was assigned as the activation energy for complexation. Energy minima were found for the inclusion complex as well as for a van der Waals complex, in which the guest is positioned outside the portal (ca. 5 Å), but attracted to the host by dispersion interactions. In the case of the charged ammonium guest the van der Waals complex becomes a true association complex, which is held together by additional ion−dipole interactions between the ammonium group and the ureido carbonyl oxygens. This affects also the mode of ingression, since the organic residue of the ammonium guest enters the cavity in the previously reported flip-flop manner.[15] The reported complexation enthalpies refer to the differential energies between the van der Waals or association complexes and the inclusion complexes.

Table 6. Calculated Included Volumes, Activation Energies, and Interaction Energies for Inclusion of Various Guests in CB6[a]

	MBA	**c6**	**c5**	**c4**	**c3**	DBH	DBO	DBOA
$V_{included}$/Å^3 [b]	89	104	86	74	56	95	111	111
ΔH_c	−10.6	−10.9	−12.1	−11.3	−9.9	−11.0	−10.1	−8.0
$\Delta H_c(H^+)$[c]	−12.6	−14.4	−17.4	−12.7	−11.5			−10.6
$\Delta H^{\ddagger}_{ingress}$	4.0	6.0	2.2	2.3	2.7	9.3	11.2	11.2
$\Delta H^{\ddagger}(H^+)$[c]	6.4	9.3	4.3	4.6	5.4			16.1

[a] All energy values in kcal mol^{-1}. [b] The volume of the ring system immersed in the CB6 cavity was taken as included volume and determined by subtracting 28 Å^3 for the volume of the aminomethyl group (30 Å^3, when protonated), where applicable. The latter volume correction was obtained by subtracting the calculated volume of DBO from the calculated volume of DBOAH$^+$. [c] Values for protonated amine.

The computed data are shown in Table 6. The absolute experimental and theoretical energies cannot be directly compared due to the neglect of aqueous solvation effects in the calculations. For example, the experimental activation energies appear to be about a factor of 2 larger than the theoretical ones (18.8 vs 9.3 kcal mol^{-1} for **c6**H$^+$ and 13.4 vs 6.4 kcal mol^{-1} for MBAH$^+$). The emphasis will therefore lie on the comparison of relative trends, assuming comparable solvation effects for the different host−guest systems. The calculation predicts an increase in the activation energy upon protonation ($\Delta H^{\ddagger}(H^+)$ values); as scrutinized in the preliminary communication,[15] this is due to the different transition state for ingression of the protonated form.

The experimental binding constants (Table 2) follow the order **c4**H$^+$, **c5**H$^+$ > **c3**H$^+$ > DBH > MBAH$^+$, **c6**H$^+$ > DBO, DBOAH$^+$. The calculated enthalpies do not correctly reflect this order, but some salient features are reproduced, e.g., the stronger binding of DBH compared to DBO and the most favorable binding for c**5**H$^+$. With respect to the kinetics of ingression (Table 2), the experimental order is **c3**H$^+$ > **c4**H$^+$ > MBAH$^+$, **c5**H$^+$ > **c6**H$^+$, DBH, and the calculated one, as anticipated from the activation energies for ingression by neglecting differential entropic effects, is **c3**H$^+$, **c4**H$^+$, **c5**H$^+$ > MBAH$^+$ > **c6**H$^+$, DBH > DBO, DBOAH$^+$. The calculated activation energies demonstrate that the ingression of the small-ring homologues is essentially unhindered and that a significant steric hindrance toward ingression arises only for **c6**H$^+$ and DBH and, most pronounced, DBO and DBOAH$^+$. Inclusion of the DBO derivatives is therefore not only thermodynamically disfavored but also expected to exhibit very slow kinetics.

Discussion

The mechanistic understanding of the complexation of organic ammonium salts by cucurbiturils is of principal interest for two reasons. First, the complexation kinetics of CB6 is much slower than that observed for host systems with unobstructed openings[5−9] like cyclodextrins or calixarenes, yet closely resembles that observed for some hemicarcerands for which the entrance of the guest is rate determining.[10,86−90] The relatively tight portals

(85) Yoon, J.; Sheu, C. M.; Houk, K. N.; Knobler, C. B.; Cram, D. J. *J. Org. Chem.* **1996**, *61*, 9323−9339.
(86) Sheu, C. M.; Houk, K. N. *J. Am. Chem. Soc.* **1996**, *118*, 8056−8070.

of CB6 can cause a sizable constrictive binding of the guest, i.e., provide a physical barrier toward complexation. This phenomenon has mainly been studied for hemicarcerands in organic solvents,[12] but apparently not for other host−guest systems in aqueous solution. Second, cucurbiturils provide two distinct supramolecular interactions, namely a hydrophobic effect, which favors inclusion of organic residues, and ion−dipole interactions at the carbonyl-laced portals, which promote binding of either the cationic sites of organic guests (ammonium salts) or of inorganic cations in the solution. This results in an interesting competition and a complex interplay between two principal binding forces (hydrophobic and ion−dipole) and two different binding partners (organic ammonium guest and inorganic cation). Thermodynamic and kinetic studies are essential to develop future applications of cucurbiturils, and to understand the complexity of supramolecular interactions from a mechanistic point of view.[59] Kinetic studies, which are facilitated for cucurbiturils by the slow guest exchange, are particularly important to identify the elementary steps in intricate complexation mechanisms.

Cavity Size. CB6 forms complexes with guest molecules as large as **c6**H$^+$ ($K = 170$ M^{-1}) and DBH (1300 M^{-1}). However, larger, virtually spherical guests such as DABCO, DBO, and DBOAH$^+$ do not form host−guest inclusion complexes with CB6, but only with the next larger homologue CB7.[54] We conclude that the cavity of CB6 and its portals are too small to allow the inclusion of these larger guest molecules. Even the attachment of an ammoniummethyl group (in DBOAH$^+$), which is geometrically well disposed to coordinate with the carbonyls of one ureido rim and should thus substantially increase the affinity, does not induce complexation.

DBH has a calculated effective volume of 96 Å^3 according to our calculations (Table 6), while that of the next larger homologue DBO is 111 Å^3. Based on the experimental results, we suggest that the "capacity" or effective volume of the CB6 cavity amounts to ∼105 Å^3, suggesting that residues as large as this volume can be complexed with a sizable binding constant, especially if they possess a spherical shape to match the concave CB6 interior. The volume of the ring system in **c6**H$^+$, which is also immersed in CB6, lies also close to this size limit (104 Å^3). The estimated cavity volume lies right within the range of 75−143 Å^3 estimated for an assumed cylindrical CB6 cavity with an assumed height of 6.0 Å and a width of either 5.5 Å (equatorial diameter) or 4.0 Å (portal diameter).[17] In contrast, CB6 has been reported to have a cavity volume of 164 Å^3 based on its X-ray crystal structure.[38,39] This higher value may be related to a different method of volume assessment, namely if the volume in the outer portal regions is added, i.e., by taking the full height of CB6 (ca. 9 Å). Each of the two portal regions is known to be able to accommodate an ammoniummethyl group with an additional volume of 30 Å, thus nicely accounting for the discrepancy (105 vs 164 Å^3).

It should be noted, however, that the binding constants of guests to CB6 cannot be predicted on the basis of the effective volume alone. For example, **c5**H$^+$ and MBAH$^+$ have very similar included volumes (86 Å^3 vs 89 Å^3), but the binding constants differ by 3 orders of magnitude (3.3×10^5 M^{-1} vs 320 M^{-1}). Expectedly, the shape and space-filling nature of the included residue is critical, while the guest polarizability (which should be higher for the aromatic guest) appears to be a less important factor. This can be rationalized in terms of the low polarizability of the guest experienced inside cucurbiturils,[54] which should greatly reduce the stabilization associated with polarizability-dependent dispersion interactions.

Constrictive Binding. The tight portals of CB6 regulate access to the inner cavity and lead to a constrictive binding. Experimentally, this is born out by the fact that the thermodynamics of complexation is not related to the kinetics in the intuitively expected manner. The former reports on the stabilization inside the cavity, while the latter reports on steric interactions with the portals during ingression. For example, the binding constant decreases with increasing guest size in the order **c4**H$^+$ > **c5**H$^+$ > **c6**H$^+$ (Table 2) which reflects an increased repulsion between the host walls and the guest. This repulsion should in a first approximation lead to a faster exit, but the opposite is found to be the case, i.e., the egression rate constant is slowest for the largest guest **c6**H$^+$ due to an increased constrictive binding. Second, while the binding enthalpy ($\Delta H°$) for **c6**H$^+$ and MBAH$^+$ is essentially the same (Table 2), the activation barrier ($\Delta H^‡$) is substantially higher for **c6**H$^+$ (by 5.4 kcal mol^{-1}). As a striking manifestation of this difference, the kinetics of exchange (Table 2) is fast on the NMR time scale for MBAH$^+$ (coalesced signals)[57] but slow for **c6**H$^+$ (separate signals), i.e., the ingression and egression rate constants differ by 3 orders of magnitude (Table 2). This can be rationalized in terms of a stronger steric hindrance of the larger **c6**H$^+$ with the portals during ingression. Third, while the thermodynamics of host−guest complexation between CB6 and **c6**H$^+$ is similar in D_2O/Na_2SO_4 as in D_2O/formic acid, the complexation process displays significantly different activation barriers (Tables 1−3). This predominant effect on the kinetics can again be rationalized if one recalls that the different cations (sodium versus protons) associate with the portals of CB6 and can cause a large effect on the kinetics (modulate the constrictive binding) without displaying a systematic effect on the thermodynamics of binding.

In essence, the constrictive binding by a host reflects a sizable activation enthalpy required to enter the cavity,[10] which can be derived from experimental and computed data:

$$\Delta H^‡_{\text{constrictive}} = \Delta H^‡_{\text{ingress}} = \Delta H^‡_{\text{egress}} + \Delta H_c \qquad (2)$$

The experimental activation enthalpies for ingression of MBAH$^+$ and c**6**H$^+$ (>10 kcal mol^{-1}, Tables 2 and 3) lie far above the apparent activation energies for solvent viscous flow in water (ca. 4 kcal mol^{-1}),[91] demonstrating that the complexation is "reaction controlled", where the required "reaction" is the widening of the tight CB6 portals. The process was also investigated by force-field calculations (Table 6). The computed constrictive binding energies, reported as $\Delta H^‡_{\text{ingress}}$, become significant (relative to solvent viscosity, >5 kcal mol^{-1}) only for the bulky guest molecules, and the values are consistently

(87) Byun, Y.-S.; Vadhat, O.; Blanda, M. T.; Knobler, C. B.; Cram, D. J. *J. Chem. Soc., Chem. Commun.* **1995**, 1825−1827.
(88) Kirchhoff, P. D.; Bass, M. B.; Hanks, B. A.; Briggs, J. M.; Collet, A.; McCammon, J. A. *J. Am. Chem. Soc.* **1996**, *118*, 3237−3246.
(89) Yoon, J.; Cram, D. J. *Chem. Commun.* **1997**, 1505−1506.
(90) Helgeson, R. C.; Knobler, C. B.; Cram, D. J. *J. Am. Chem. Soc.* **1997**, *119*, 3229−3244.
(91) Cho, C. H.; Urquidi, J.; Singh, S.; Robinson, G. W. *J. Phys. Chem. B* **1999**, *103*, 1991−1994.

Scheme 1

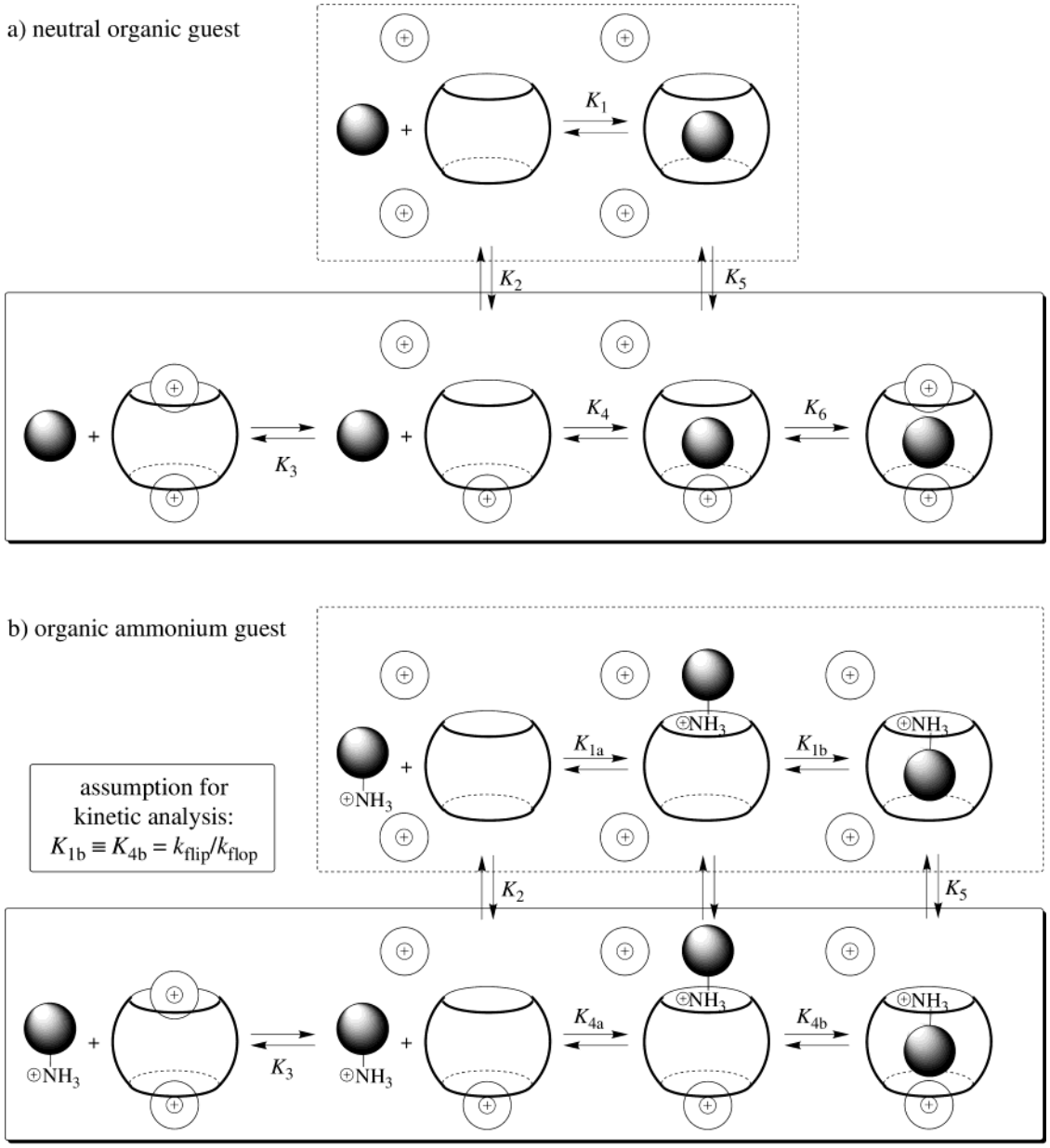

largest for those guests (>10 kcal mol^{-1}), for which no binding is experimentally observed. Note that the constrictive binding computed for some potential guests (ca. 16 kcal mol^{-1} for DBOAH$^+$) resembles that calculated for some hemicarcerands.[86,92]

Complexation Mechanism. The sequences of elementary reactions shown in Scheme 1 present the simplest kinetic scenarios consistent with our current understanding of CB6 guest complexation and, in particular, the presently reported findings. The mechanism in Scheme 1a applies to small uncharged guests and that in Scheme 1b to organic guests with suitably positioned ammonium cation sites (e.g., ammoniummethyl groups). CB6 is well-known to complex protons and metal cations, which are not enclosed but which associate to the portals of CB6.[19,35,58,67,68] In fact, CB6 *requires* the presence of cations (generally protons or alkali cations) to dissolve in sufficient (mM) quantities in water (reactions in bold frame). On the other hand, the solubility of uncomplexed cucurbit[6]uril is not sufficiently low (ca. 30 μM) to ignore it in the detailed complexation mechanism (reactions in dashed frame). The cations form either 1:1 or 2:1 complexes with cucurbit[6]uril, since the cations can complex with one or two of the portals; an equilibrium between these two species must be considered. Higher order complexation patterns (4:1) have been suggested,[58] based on crystallographic data,[19] but are not required to account for the reported solution data[20,41] and seem unlikely in view of the resulting charge repulsion at the same rim. Note that our mechanistic scheme, in contrast to the complexation scheme proposed by Hoffmann et al.,[62] involves also the ternary complex, CB6·guest·M$^+$, in which the ammonium group and the metal cation are bound simultaneously to opposite portals (bottom right structure in Scheme 1b). As revealed by NMR data (see Results), the cyclohexyl ring of **c6**H$^+$ is centered in the core of CB6 and

(92) Nakamura, K.; Sheu, C. M.; Keating, A. E.; Houk, K. N.; Sherman, J. C.; Chapman, R. G.; Jorgensen, W. L. *J. Am. Chem. Soc.* **1997**, *119*, 4321−4322.

Scheme 2

$$\mathrm{CB6} + \mathbf{c6}\mathrm{H}^{\oplus} \overset{K_1}{\rightleftharpoons} \mathrm{CB6}\cdot\mathbf{c6}\mathrm{H}^{\oplus} \quad \text{(a)}$$

$$\mathrm{CB6} + \mathrm{M}^{\oplus} \overset{K_2}{\rightleftharpoons} \mathrm{CB6}\cdot\mathrm{M}^{\oplus} \quad \text{(b)}$$

$$\mathrm{CB6}\cdot\mathrm{M}^{\oplus} + \mathrm{M}^{\oplus} \overset{K_3}{\rightleftharpoons} \mathrm{CB6}\cdot 2\mathrm{M}^{\oplus} \quad \text{(c)}$$

$$\mathrm{CB6}\cdot\mathrm{M}^{\oplus} + \mathbf{c6}\mathrm{H}^{\oplus} \overset{K_4}{\rightleftharpoons} \mathrm{CB6}\cdot\mathbf{c6}\mathrm{H}^{\oplus}\cdot\mathrm{M}^{\oplus} \quad \text{(d)}$$

$$\mathrm{CB6}\cdot\mathbf{c6}\mathrm{H}^{\oplus} + \mathrm{M}^{\oplus} \overset{K_5}{\rightleftharpoons} \mathrm{CB6}\cdot\mathbf{c6}\mathrm{H}^{\oplus}\cdot\mathrm{M}^{\oplus} \quad \text{(e)}$$

should not interfere with metal ion binding to the vacant portal; this view is supported by molecular modeling.[15]

As proposed by Kim and co-workers,[19,58] the cations may serve as "lids", which block the passage, both on a pictorial as well as on an elementary mechanistic level, of the guest through the portals. An uncharged guest may enter the cavity directly (Scheme 1a), but an organic ammonium cation will first coordinate with the portal to form an association complex, and the organic moiety will enter the cavity in a second step (Scheme 1b). This recently reported mechanistic detail provides an explanation for the experimentally observed pH-dependent kinetics.[15] If the guest is an organic ammonium ion, the ammonium group will subsequently block one portal and prevent a second proton or alkali cation from associating. In the case of the uncharged guest, a second cation may associate with the vacant portal after complexation, thus forming a "supramolecular barrel" with a top and bottom lid (Scheme 1a).

Thermodynamics of Complexation. To study the complexation mechanism experimentally, we have chosen **c6**H^+ as guest, which allows the accurate determination of both binding constants and rate constants due to its intermediate affinity to CB6 and the slow exchange. The association complex of the ammonium ion in Scheme 1b is required to account for the experimental kinetics in this case, but does not affect the *thermodynamics* since it is in fast preequilibrium with "empty" CB6 and **c6**H^+.[15] The microscopic binding constants K_{1a} and K_{1b}, as well as K_{4a} and K_{4b}, in Scheme 1b may therefore be replaced by macroscopic binding constants K_1 and K_4, which represent the product of the two corresponding microscopic binding constants. The quantitative analysis of the *thermodynamic* data is then represented by the five equilibria in reactions a−e in Scheme 2 with M^+ representing a metal ion. Note that the binding constant K_5, which measures the affinity of the CB6·**c6**H^+ complex for the sodium, is a dependent one and equals K_2K_4/K_1. The macroscopic binding constant K_1 could be independently determined ($1.1 \times 10^5\ M^{-1}$, cf. the Experimental Section) through the solubilization of solid CB6 in the presence of an excess of **c6**H^+ and the independently determined solubility of CB6 (30 μM) in pure water, i.e., in the absence of metal cations.

The expression for the NMR-spectroscopically determined equilibrium constant in the presence of sodium cations is given by eq 3. Equation 3 takes into account that NMR is sufficiently fast to differentiate between host molecules with (numerator in eq 3) and without (denominator in eq 3) included guest, but too slow to differentiate between host molecules with and without associated sodium (sums in the numerator and denominator). This situation results in the characteristic two sets of resonances in the NMR spectra.

Table 7. Equilibrium Constants (M^{-1}) for the Elementary Reactions Involved in the Inclusion of **c6**H^+ in CB6 As Deduced from Experiments at Different Salt Concentrations and Fitting Procedures According to Scheme 1 and eq 4

parameter set	K_1 [a]	K_2	K_3	K_4	K_5
statistical[b]	1.1×10^5	3120	780	5.0×10^4	1560
experimental[c]	1.1×10^5	≡ 1450	≡ 60	3820	55

[a] Experimental value, see text. [b] Assuming $K_1 \equiv 2K_4$ and $K_2 \equiv 4K_3$, cf. ref 93. [c] K_2 and K_3 values in water/formic acid taken from ref 62.

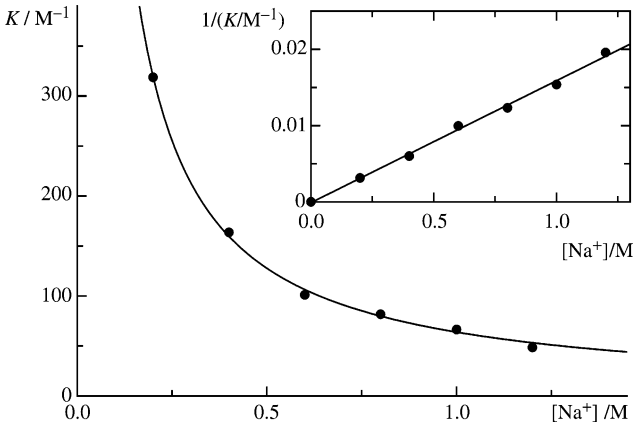

Figure 3. Plots of the binding constant for the CB6·**c6**H^+ complex versus sodium cation concentration in D_2O and fits according to eq 4 (statistical parameter set from Table 7) or eq 5 (inset).

$$K = \frac{[\mathrm{CB6}\cdot\mathbf{c6}\mathrm{H}^+] + [\mathrm{CB6}\cdot\mathbf{c6}\mathrm{H}^+\cdot\mathrm{M}^+]}{[\mathbf{c6}\mathrm{H}^+]([\mathrm{CB6}] + [\mathrm{CB6}\cdot\mathrm{M}^+] + [\mathrm{CB6}\cdot 2\mathrm{M}^+])} \quad (3)$$

Substitution of the binding constants for reactions a−d in Scheme 2 into eq 3 and consideration of the large excess of added salt (>200 mM) relative to 3 mM host ($[Na^+] \approx [Na^+]_o$) yields eq 4 as an analytical expression for the anticipated dependence of the experimentally observed equilibrium constant on the cation concentration.

$$K_{\mathrm{obs}} = \frac{K_1 + K_2K_4[\mathrm{M}^+]}{1 + K_2[\mathrm{M}^+] + K_2K_3[\mathrm{M}^+]^2} \quad (4)$$

Nonlinear least-squares fitting of the experimental sodium concentration dependence to eq 4 by employing the known value for K_1 (see above) is possible, but the errors turn out to be large and correlated. The fitting was therefore performed within two sets of alternative constraints (Table 7, Figure 3). The first set assumes a purely statistical relationship between the binding constants,[93] namely $K_1 \equiv 2K_4$ and $K_2 \equiv 4K_3$, which takes into account the number of binding sites available for association and dissociation; this approach ignores a possible repulsion between the remote cationic sites at opposite portals. The second set makes use of experimental binding constants reported by Hoffmann et al. for the association of the first and second sodium ion.[62] Regardless of the large variations in the fitted parameters between the two data sets (Table 7), the ratio of K_4/K_3, which reveals by which factor the ammonium inclusion complex is more stable than the sodium complex, is accurately

(93) Connors, K. A. *Chemical Kinetics: The Study of Reaction Rates in Solution*; John Wiley & Sons: New York, 1990.

defined (64 ± 1). Note also that the value of K_5 does not fall below the value of K_3 for both sets of data. This indicates that there is no substantial steric repulsion between the included organic residue (cyclohexyl ring) and the sodium cation associated to the second portal (see the complexation mechanism in Scheme 1b).

Effect of Metal Ions on the Binding Constant. The absolute values resulting from fitting (Table 7) along with the practically useful range of salt concentrations (≥0.1 M) justify two further approximations in the denominator and numerator of eq 4, namely $K_1 + K_2K_4[M^+] \approx K_2K_4[M^+]$ and $1 + K_2[M^+] + K_2K_3[M^+]^2 \approx K_2[M^+] + K_2K_3[M^+]^2$. The simplified expression in eq 5 is then obtained, which is useful to predict the effect of competitive metal ion binding: The binding constants of organic ammonium salts is expected to decrease linearly with increasing salt concentration [M^+], or likewise with increasing cation binding constant (K_3). From a mechanistic point of view (Scheme 1), an increase in either [M^+] or K_3 decreases the amount of host with at least one uncomplexed portal, which is essential for guest complexation. Indeed, the binding constant of c**6**H^+ is largest in the presence of the larger alkali ions, which have a lower affinity to CB6 (Table 5). In addition, there is a linear relation between $1/K_{obs}$ and [M^+] for sodium ions (inset in Figure 3), as expected from eq 5.[94]

$$\frac{1}{K} = \frac{1}{K_4} + \frac{K_3}{K_4}[M^+] \qquad (5)$$

The adjustment of the salt concentration and the type of salt provides a tool to control the thermodynamics of complexation and to vary the binding or release of guests at will with quantitatively predictable outcome.[95] A similar conclusion has recently been reached by Moon and Kaifer for the effect of metal cations on the binding of viologen guests by CB7,[52] which can presumably be treated within a similar framework as that provided by Schemes 1 and 2 herein.

The "true" binding constant of c**6**H^+ by CB6, i.e., K_1 in pure water, is 3 orders of magnitude higher than that determined in the presence of sodium cations (Table 4). K_1 is also 2−3 orders of magnitude higher than the binding constants of NH_4^+ (170 M^{-1}) and Na^+ (1450 M^{-1}) to one portal of CB6,[62,83] which demonstrates that hydrophobic host−guest interactions[60] contribute significantly to the complexation, in addition to the ion−dipole interaction with the RNH_3^+ cationic site. The importance of hydrophobic effects (which include the release of high-energy water from the host cavity) is also born out by the sizable binding of neutral guests such as DBH (Table 3), and the previously observed weak binding by the uncharged *amine* form, **c6** ($K = 10$ M^{-1}, Table 3).

The presently observed decreased binding of an organic ammonium ion with increasing cation concentration is in contrast to previous reports according to which sodium cations serve as "lids" of CB6, which assist the binding of neutral organic guests, e.g., tetrahydrofuran.[19,58] Presumably, the alkali ions stabilize this complex not by providing a physical barrier toward exit, but by providing an additional stabilization through ion−dipole interaction with the oxygen lone pairs of the ether. The removal of the sodium ions by addition of acid, i.e., competitive binding of protons to the portals, removes this stabilization, and eventually leads to a dissociation of the destabilized host−guest complex.

Kinetics of Complexation. The evidence for constrictive binding of c**6**H^+ by CB6 requires the rate-determining step for both ingression and egression to be the unimolecular interconversion of the association to the inclusion complex. Let us assume that this rate-determining process is independent of the presence of the cation complexed to the other end, i.e., $K_{1b} \equiv K_{4b} = k_{flip}/k_{flop}$ in Scheme 1b.[15] The reversible formation of all association complexes occurs rapidly. Preequilibrium kinetics then applies, which allows one to derive an analytical expression for the ingression rate constant according to eq 6a. The expression can be further simplified (eq 6b) by imposing the statistical assumptions on the binding constants, i.e., $K_{1a} \equiv 2K_{4a}$ and $K_2 \equiv 4K_3$, and by assuming $2K_2[M^+] \gg 1$ as a consequence of the large cation binding constant (Table 7) and the selected metal ion concentration (≥0.1 M).

$$k_{ingress} = k_{flip}\frac{K_{1a} + K_2K_{4a}[M^+]}{1 + K_2[M^+] + K_2K_3[M^+]^2} \qquad (6a)$$

$$k_{ingress} \approx \frac{2k_{flip}K_{1a}}{K_2[M^+]} \text{ for } K_2[M] \gg 1, \text{ with } K_{1a} \equiv 2K_{4a}, \text{ and } K_2 = 4K_3 \qquad (6b)$$

The experimentally measured ingression rate constant should accordingly *decrease* with increasing cation binding constant (K_2) and the cation concentration according to eq 6b. The observed variations with the alkali cation concentration (Table 4) and the cation type/size (Table 5) are in agreement with this simple kinetic model, since they reveal a decrease of the ingression rate constant with an increase in either metal concentration or cation binding constant. Within the approximations made, the egression rate constant ($k_{egress} = k_{flop}$) should be *independent* of the cation binding constant or concentration. This is reflected, in particular, in the experimental data in Table 4, where the egression rate constant remains essentially constant with increasing sodium ion concentration. By assuming a constant egression rate constant, it is also possible to extrapolate the ingression rate constant to pure water (Table 4). Again, like it is the case for the binding constants, the ingression rate is expected to be much larger in the absence of cations as a consequence of the complexation mechanism (Scheme 1).

Conclusions

The present study on host−guest complexation by cucurbit[6]uril has demonstrated that the inner cavity has a guest capacity of ca. 105 Å^3, which corresponds to residues with up to 7 heavy atoms, or guests as large as cyclohexylmethylammonium and 2,3-diazabicyclo[2.2.1]hept-2-ene. The comparison of kinetic and thermodynamic data, as well as force-field calculations, corroborates the existence of a sizable constrictive binding. This means that the ingression into the cavity requires

(94) Although the slope of the fit according to eq 5 is well defined and can be used to obtain the ratio of K_4/K_3 (see above), the fit cannot be reliably used to extract the individual values of K_4 and K_3 because the intercept has a large error and slope and intercept are correlated.

(95) When Scheme 3b is used to model the experimental binding behavior in the presence of protons (acid) instead of sodium cations, a satisfactory fit was not possible in the very low pH region, where protonation of CB6 occurs. A more complex mechanism seems to apply in this case, which may involve more than one proton per portal (cf. ref 82). However, the qualitative effect, i.e., weaker binding of the guest upon protonation of CB6, remains the same.

a substantial activation barrier, which is due to the required widening of the tight portals of this molecular container compound. The investigation of the effect of metal ions has allowed a detailed understanding of the complexation mechanism (Scheme 1), which involves an explicit consideration of cations associated to the carbonyl rims. Accordingly, the thermodynamics and kinetics of binding of ammonium ions can be fine-tuned not only through the proper choice of pH, as described in the preliminary communication,[15] but also through the choice of the cation type and, more importantly, the cation concentration. The binding constants as well as the ingression rate constants decrease with the inverse of the cation concentration and cation binding constant, while the egression rate constants are less affected. Thus, most thermodynamic and kinetic data reported for CB6 until now do not truly reflect the inherent affinity between host and guest, but report mostly on the presence of metal cations or protons. Care must therefore be taken in the comparison of reported binding constants. The strong and predictable response of host−guest complexation to the presence of metal ions is also of interest for practical applications of cucurbiturils, e.g., the removal of contaminants from water.

Acknowledgment. We are most grateful for financial support by the Swiss National Science Foundation (Project Nos. 620-58000.99 and 4047-0575552) within the program NRP 47 "Supramolecular Functional Materials". R.R.H. thanks the National Science Foundation (U.S.A.) for an International Research Fellowship (Grant No. INT-9901459).

JA0319846